SIMULATION OF HELICOPTER VIBRATION REDUCTION BY MEANS OF HIGHER HARMONICS CONTROL WITH THE USE OF FLIGHT SIMULATOR

Samusenko A.G., asamusenko@mi-helicopter.ru
Esaulov S.Yu., sesaulov@mi-helicopter.ru
Ivchin V.A., vivchin@mi-helicopter.ru

Mil Helicopter Plant JSC
Russia
140070, Moscow Region
Tomilino, 26/1 Garshina St.

Key words: Vibrations, Multicyclic control, Hub shears and moments, Flight simulator.

Abstract: This paper describes a preliminary phase of the program is being launched by Mil Design Bureau (MDB) on the development of multicyclic control system for the production Mi-8 helicopter. The investigation of multicyclic Mi-8 rotor control according to the IBC concept was made with the use of MDB flight simulator with comprehensive mathematical model of the rotor and helicopter dynamics. This model was used to determine high frequency response of hub shears and moments to the multicyclic input signals. The influence on 4/rev, 5/rev, and 6/rev multicyclic harmonics on the dominating 5/rev content of hub shears and moments was evaluated. Multicyclic amplitudes were imposed in the form of equivalent pitch angle of each rotor blade.The data obtained are pertinent to evaluate the applicability of the rotor/helicopter model for multicyclic control investigations, and evaluate by the first approximation the influence of various input harmonics on the 5/rev hub shears and moments content.

1. INTRODUCTION

The helicopter as unsurpassed by its performance VTOL flight vehicle firmly took its place in the world aviation. From the first production rotorcrafts in 1950s to the present time all helicopter flight performance items were improved sighnificantly. But some “inborn” helicopter shortcomings still prejudice their effective usage. In the first place this is relatively high level of vibrations, well above the same for fixed wing aircraft, caused by aerodynamic environment in forward flight. Attempts to lessen helicopter vibrations began almost immediately after the real rise of helicopter operations [1-6]. Two main ways to solve this problem were established: passive and active methods [21]. Passive methods based on the rational design and on the usage of various vibrations isolation means soon gave perceptible results, but now it may be stated that the potential of these methods is exhausted. The vibration level as low as 0.1g was reached, but further vibration reducing by passive means seems to be impossible.

The second way – active approach - also

appeared in 1950-60s. Two concepts were distinguished: HHC (multicyclic commands input via swashplate), and IBC (multicyclic commands input to each blade). Electro-hydraulic servo units were used in both concepts: to obtain high frequency response for such units was a serious problem. Up to the end of 1990s a great amount of theroretical investigations, wind-tunnel experiments [10,11,15,17] and even some flight tests [7-9] were conducted with both concepts, but further their realization did not continue because of the extreme complexity of such systems.

The situation changes dramatically with the advent of so called “smart” materials, firstly piezoceramic materials: on this base it was possilble to create light and compact actuators which are able to generate mechanical control signal of very high frequency [12,13]. This idea created a plurality of active devices[14,20,22,23]. The most effective active vibration control was implemented by active trailing edge blade flaps with the piezoceramic actuators [16,24]. Successful vibration reduction, up to 90% with this method was demonstrated in flight by Eurocopter Deutschland at the BK-117 helicopter [18,18,21].

MDB from 2009 has launched a program on the development of multicyclic control system for reduction of helicopter vibration. The program include a feasibility study of creating such a system for the production Mi-8 helicopter. On the preliminary phase the investigation of multicyclic Mi-8 rotor control according to the IBC concept was made with the use of MDB flight simulator with comprehensive mathematical model of the rotor and helicopter dynamics. This model was used to determine high frequency response of hub shears to the multicyclic input signals. In this paper was investigated the influence on 4/rev, 5/rev, and 6/rev multicyclic harmonics on the dominating 5/rev content of hub shears amd moments. Multicyclic amplitudes were imposed in the form of equivalent pitch angle of each rotor blade.

2. TASK FORMULATION

At the preliminary phase of the work, after studying of various theoretical papers on this topic, it was decided to evaluate the applicability of the known theoretical preconditions for the multicyclic control to the real task of suppresion the Mi-8 helicopter vibrations.

It is known from experimental and analytical studies that predominant sourse of periodic loads on a helicopter is a blade passage frequency f_b which is a product of rotor frequency and number of blades. Figure 1 depicts an experimental vibration spectrum in vertical and lateral planes at CG for a medium size helicopter with 6-bladed rotor at cruise flight airspeed. The blade passage frequency in this case equals to 19.4 Hz. It is seen that maximum vibration amplitude corresponds to this frequency.

It is also known that in rotating coordinate frame the sourses producing vibration with blade passage frequency in nonrotating frame correspond to frequencies of f_b, $f_b \pm 1$

So in the present study it was necessary to determine how the hub periodic shears and moments of dominating 5/rev harmonic change with input of various 4/rev, 5/rev, and 6/rev harmonics amplitudes and phases. To solve this task it was decided to use the rotor model describing articulated rigid blade motion relative to flap and lead-lag hinges together with the helicopter dynamics. This rotor/helicopter model was implemented in the MDB Flight Simulator.

It was also necessary to evaluate the applicability for this case of the quasi-stationary rotor model with representation of rotor in the form of “Transfer Matrix” created by several authors (McCloud, Shaw, Johnson, et al), for example, in Ref.[1,5,6].

3. MATHEMATICAL MODEL OF ROTOR/HELICOPTER IN THE FLIGHT SIMULATOR

To solve problems of the rotor multicyclic control was used the MDB Flight Simulator with a non-linear helicopter mathematical model proceeding in the real time frame. Main features of this model, opposite to those commonly used in flight simulators, are the non-linear models of main and tail rotors. Earlier were used linear rotors models, or at the best case, grid models where rotors parameters were given in the form of linear equations coefficients, or models with static rotors parameters preliminary calculated for the required range of flight regimes. The rotors models used in this study were based on the direct computation of instant rotor parameters with the integration of the each blade motion together with the integration of the helicopter motion as a whole. This approach is of principal significance with application to multicyclic rotor control problems.

In the helicopter model, instead of static rotor parameters interpolation, are included generic computational programs for integrating the each blade motion in the real time frame. This approach allows to remove practically all assumptions pertinent to grid rotor models, and to obtain the whole helicopter dynamics with the inclusion of main and tail rotor dynamics.
Figure1 represents a structure of the helicopter model in the flight simulator.

The main advantages of the new rotor models are as follows.

- Rejection of the equivalent rotor theory.
- Rejection of quasi-steady approach and preliminary computation of static rotor parameters.
- Computation of rotor hub shears and moments caused by all helicopter motion parameters.
- Precision computation of rotor parameters influenced by changes of rotor rpm and atmospheric environment.
- Possibility to use of modern methodology for computations on rotor blade aerodynamics, structural issues and stability in real time, with inclusion of human pilot activity.
- Possibility to realize any rotor control algorithm in real time with analysis of vibration in any point of fuselage.

The main and tail rotor induced velocities are modelled on the base of Mangler and Squaire disc theory [26]. Ground effect is modelled on the base of Shaidakov and Artamonov disc theory [27,28].

In computations are used airfoils aerodynamics data obtained in experiments with TSAGI wind tunnels in steady and unsteady environment and for sweep wings [29].

In the fully articulated rotor model the blade motions relative to flap, lead-lag and feathering hinges are considered. The blades are assumed to be rigid in bending and torsion. Integration of blade flap and lead-lag motion is performed with taking into account a change of blade feathering depending upon blade azimuth angle in forward flight. Dedicated software was created for a model of lead-lag damper.

Figure 2 represents examples of time histories of the flap and lead-lag blade motions at the initial phase of forward flight computation. Main curves represent 7 initial rotor revolutions, on the upper right corners are presented the time histories for all computational sample. In the main and tail rotors software the time step is chosen to be in compliance with blade azimuth angle change not more thah 10 degrees.

Other feature of the helicopter model is an inclusion of a power plant model. This model contains two turboshaft engines together with main/tail rotors and geardox interconnected by elastic transmission (Figure 3).

This power plant model improves accuracy of high frequency loads computations especially in transient modes in the case of one or two engines failure. The power plant model implementation gives more accuracy to blade motions computation.

According to the task of this study the model of helicopter flight control system includes all real kinematical parameters and a model of an autopilot installed on this helicopter. Multicyclic control is entered by insertion in feathering angle of each blade additional quantities with given parameters or with parameters determined in forward flight in accordance with:

$$\begin{aligned}\Delta\varphi_i &= a_{n-1}\sin(n-1)\psi_i + b_{n-1}\cos(n-1)\psi_i + \\ &+ a_n \sin n\psi_i + b_n \cos n\psi_i + \\ &+ a_{n+1}\sin(n+1)\psi_i + b_{n+1}\cos(n+1)\psi_i\end{aligned} \qquad (1)$$

Where:

$\Delta\varphi_I$ – incremental feathering angle of i-th blade;

ψ_I - azimuth angle of i-th blade;

n – number of rotor blades;

a, b – coefficients of corresponding control harmonics.

4. RESULTS OF PARAMETRICAL INVESTIGATIONS

Initial investgations were conducted for the Mi-8 helicopter at level flight with airspeed of 150 km/h. The flight simulator was used to establish steady level flight and to obtain vibration spectra at the helicopter CG, which are depicted in Figure 5. The spectra show that the frequency of dominant vibration corresponds to blade passage frequency, 16 Hz with the rotor speed of 3.2 Hz (20.1 rad/sec) for the Mi-8 helicopter.

Then at steady flight regime a multicyclic control was entered by insertion in feathering angle of each blade the IBC signal:

$$\Delta\varphi_i=0.5°\sin[n\cdot(\omega\cdot t+i\cdot\Delta\psi)+\Phi], \qquad (2)$$

where i- number of harmonic (4/rev, 5/rev, 6/rev), Φ - control phase (0°…360°)

In the investigation there are considered hub shears and moments in the helicopter body axes coordinates as follows:

T – thrust;

S – lateral shear;

H – longitudinal shear;

Mx – lateral moment;

My – yaw moment;

Mz – longitudinal moment

The results of investigation for 4/rev, 5/rev, and 6/rev control efforts are showed on Figures 6, 7, and 8 respectively. Control amplitude was 0.5° for all cases, phase changes were conducted discretely, per every 3 rotor revolutions, with increase by 12° after each step.
These figures represent time histories of three hub shears and three hub moments.

From the results obtained it may be concluded that yaw moment My is practically independent on the control harmonic number and phase. Also from consideration of curves stems the conclusion than minimum amplitude values of hub shears and moments correspond to various control phases.

Then FFT analysis was performed to determine 5/rev shears and moments content for each time interval corresponding to three rotor revolutions for each control phase value.

Figures 8, 9, and 10 represent results of this analysis in the form of 5/rev content for three generalized loads acting relative to the helicopter CG for various control phases. The generalized loads are as follows:

$F_{\Sigma} = \sqrt{(S^2+H^2)}$ – summary shear acting in lateral plane of body axes (in-plane shear).

$M_{\Sigma} = \sqrt{(M_x^2+ M_z^2)}$ – summary moment in vertical plane acting relative to CG.

Y – Summary vertical force (thrust).

Summary shear F_{Σ} and summary moment M_{Σ} are vectors in the rotating coordinate frame with the amplitude depending upon azimuth angle. The amplitude variation is caused by non-linear variations of shears and moments generating by main rotor, fuselage, empenange, tail rotor, power plant, etc.

The results of analysis show the influence of multicyclic control on the periodic loads and determine the control phase corresponding to the mimimum of each load. Baseline loads (without multicyclic control) are shown for comparison.

The optimal effect of multicyclic control is achieved by means of 4/rev harmonic (number of blades minus 1). In this case the minimal loads are achieved practically at the same control phase of approximately 290°.

It can be seen from the graphs on Figure 10 that 5/rev control harmonic has practically no effect on summary F_{Σ} shear and summary M_{Σ} moment. The control phases for minimum in-plane shears are shifted by approximately 150°, at the same time the thrust component has raised at least 3 times.

Control with 6/rev harmonic (Figure 11) lessen significantly the thrust component, but decrease in the summary shear and moment are less than the same for 4/rev harmonic (2 times less for the shear, and 4 times less for the moment).

Figures 12-14 depict the results in some another form, namely in the form of load vectors loci. The results are shown for baseline case, and for multicyclic control with 4/rev, 5/rev, and 6/rev harmonics. The control phases corresponding to minimum 5/rev thrust are respectively 288° , 36° , and 96°. It is seen that, due to non-linearity of the helicopter model, the loci for summary shear and moment are not exact circles. The graphs show explicitly a decrease or an increase of 5/rev loads harmonic. Similar results are obtained for airspeeds of 230 and 300 km/h. For comparison, Figure 15 and 16 depict the results for airspeeds of 230 and 300 km/h, with 4/rev control similar to those on Figure 12 (Figure 15 shows the loads loci for 230 km/h, and Figure 16 for 300 km/h). Analogous results are obtained for these airspeeds with 5/rev and 6/rev control.

Comparing the graphs on Figures 15 and 16 with those of Figure 12, one can see that the baseline loads amplitudes increase significantly with growth of airspeed. For better view Figure 17 shows comparable graphs of 5/rev loads vs. 4/rev control phase for airspeeds of 150, 230, and 300 km/h. Mean baseline loads amplitudes are shown by dotted lines. One can see that 5/rev shear and moment, together with baseline values, increase practically linearly vs. airspeed, but 5/rev thrust raises 3 times comparing to baseline.

The graphs show also that 4/rev control efficiency increases vs. airspeed, the optimal control phase also increases slightly.

Comparing the graphs on Figures 12, 15, and 16, one can see, that loci for in-plane shear and for summary moment change with an increase of airspeed becoming more elliptical, i.e. the longitudinal and lateral shears are decreased, but the diagonal in-plane shear is increased.

It shall be noted that the maximum values of in-plane shear and summary moment practically lay in mutually perpendicular planes.

In all previously investigated cases the multicyclic amplitude was constant (0.5°). Then the influence of multicyclic amplitude changes on 5/rev loads was investigated. For example, in this paper is presented a result of 4/rev amplitude changes at airspeed of 230 km/h.

Figure 18 depicts the 5/rev loads vs. control phase for three values of control amplitude. It is seen that the increase of amplitude corrersponds to almost proportional decrease of minimum 5/rev in-plane shear and summary moment (control phase = 300°). Minimum thrust value is increased.

On Figure 19 are shown load vectors loci for 4/rev control with three amplitude values and phase of 300°. It is seen that loci for in-plane shear and for summary moment with an increase of airspeed degenerate from elliptical form into almost strait lines, i.e. the longitudinal and lateral shears are practically nullified.

The results obtained mean that the efficiency of multicyclic control with 4/rev, 5/rev, and 6/rev harmonics vary significantly for various amplitudes and flight regimes. Consequently, these harmonics shall be used in proper combinations to obtain an optimal vibration control directly at any flight regime

5. RESULTS OF INVESTIGATIONS ON OPTIMIZATION

For investigation of combined control with 4/rev, 5/rev, and 6/rev harmonics, the dedicated sofware was elaborated using an approach of transfer matrix (T-matrix)[1,5,6,10]. The main rotor model was considered in the form:

(3) $$Z = Z_0 + TU$$

where:
Z – vector of rotor output (periodic 5/rev components of total hub shear and moment relative to the helicopter CG) with multicyclic control applied in the form of sin amd cos components;
Z_0 - vector of rotor output without multicyclic control;
T - transfer matrix (6 x 6 dimension in this case) setting a relationship between harmonic pitch inputs abd harmonic components of vibratory hub loads;
U – multicyclic control vector (sin and cos components of 4/rev, 5/rev, and 6/rev harmonics).

The T-matrix can be determined by least square method: obtaining a number (N) of input/output quantities, and applying a formula:

…(4)… $T = \check{Z}\acute{U}^T(\acute{U}\acute{U}^T)^-$

where:
Ž, Ú - matrices comprising of N rows, each of row represents a sample of input/output measurement (index "T" means transpose, index "-1" means inversion).

Minimum value of N should be 2-3 times more than dimension of vector U, in this paper N = 24. To realize this algorithm a random number generator was used for obtaining sin and cos multicyclic control components for 4/rev, 5/rev, and 6/rev harmonics. Each measurement sample was executed in the time interval of three rotor revolutions. Then the software was implemented into the flight simulator helicopter model, and its functionality was evaluated. The input samples in terms of amplitudes and phases used in the T-matrix determination are presented in Figure 20.

Then optimal control was applied in accordance with well-known LQG technique:

(5) $$Uopt = CZ$$

where:

(6) $C = -DT^T$ - optimal control gains matrix;

(7) $D = (T^T QT + R)^{-1}$.

The weighting matrices Q (for quality of control) and R (for input constraint) were properly chosen after some iterations.

The results of optimal control application are depicted on Figures 20 and 21. On Figure 20 the optimal amplitudes and phases for each control harmonic are presented with dotted lines. Table 1 represents the same data.

Table 1

Optimal control	Amplitude deg.	Phase deg.
4/rev	1.187	-68.0
5/rev	0.245	138.4
6/rev	0.712	-27.0

On Figure 21 are presented time histories of vibratory loads for baseline case (no multicyclic control) at initial time interval (t = 0 – 4.5 sec.), at medium time interval (24 samples for T-matrix determination, t = 4.5 – 26.7 sec.), and at time interval of optimal control application (t = 26.7 – 33.0 sec.).

Table 2 represents reduction of 5/rev vibratory loads due to the optimal control.

Table 2

	% of Vibratory Loads Reduction	
	Moment	Shears
X-axis	81.5	90.7
Y-axis	28.6	58.3
Z-axis	71.4	79.6

The most reductions are for in-plane shears and moments in vertical plane, thrust component reduction is less.

It is necessary to note that the presented investigation is dealt with rotor blades rigid in bending and torsion. Accounting for blade aeroelasticity can change the obtained results in quantitative sense, but principal changes seem to have low probability.

6. CONCLUSIONS

(1) The investigations were carried out on the multicyclic vibrations control with the MDB flight simulator using non-linear mathematical model of the Mi-8 helicopter.

(2) Parametrical investigations show that for 5-bladed Mi-8 helicopter rotor the most effective multicyclic control includes 4/rev harmonic.

(3) With the use of flight simulator was elaborated an algorithm for in-flight determination of T-matrix with subsequent obtaining LQG gains for optimal control.

7. REFERENCES

[1] Shaw, J., Albion, N. "Active Control of Rotor Blade Pitch for Vibration Reduction: A Wind Tunnel Demonstration". Vertica v.4, pp. 3-11. 1977.

[2] Yen, J.G. "Higher Harmonic Control for Helicopters with Two-Bladed and Four-Bladed Rotors". J. Aircraft v.18, No.12, 1980.

[3] Yen, J.G. "Vibration Reduction with Higher Harmonic Blade Feathering for Helicopters with Two-Bladed Teetering and Four-Bladed Hingeless Rotors". American Helicopter Society Preprint No. 80-69, 1980.

[4] Reichert, G. "Helicopter Vibration Control – A Survey". Vertica v.5, pp. 1-20, 1981.

[5] Johnson, W. "Self-Tuning Regulators for Multicyclic Control of Helicopter Vibration". NASA Tech. Paper No. 1996, 1982.

[6] Chorga, I., McLoud III, J.L. "A Numerical Simulation Study of Open-Loop, Closed-Loop and Adaptive Multicyclic Control Systems". Univ. of Maryland, NASA

Ames, American Helicopter Society Meeting on Helicopter Vibration, 1982.
[7] Polychroniadis, M., Achache, M. “Higher Harmonic Control: Flight Test of an Experimental System On SA 349 Research Gazelle”. 42nd Annual Forum, American Helicopter Society,Proccedings, pp. 811-819, 1986.
[8] Miao, W., Kottapalli, S.B.R., Frye, H.M. “Flight Demonstration of Higher Harmonic Control (HHC) on S-76”. 42nd Annual Forum, American Helicopter Society, Proceedings, pp.777-791, 1986.
[9] Walsh, D.M. “Flight Test of an Open Loop Higher Harmonic Control System on an S-76A Helicopter”. 42nd Annual Forum, American Helicopter Society, Proceedings, pp.831-843, 1986.
[10] Nygren, K.P., Schrage, D.P. “Fixed-Gain vs. Adaptive Higher Harmonic Control Simulation”. J. American Helicopter Society, v.34, 1989.
[11] Muller, M. et al. “On the Importance and Effectiveness of 2/rev IBC for Noise, Vibration, and Pitch Link Load Reduction”. 25th European Rotorcraft Forum, Paper G4, 1999.
[12] Giurgiutiu V. “Recent Advances in Smart Material Rotor Actuation.. AIAA Paper 2000-1709, 2000.
[13] Toulmay, F., Kloppel, V., Lorin, F., Enenkl, B., Gaffiero, J. “Active Blade Flaps – The Need and Current Capabilities”.. 57th Annual Forum American Helicopter S0ciety, 2001.
[14] Bernhard, A.P.F., O’Neill, J., Kohlhepp, F., Welsh, W., Lorber, P. ‘‘Active Rotor Control (ARC) of a Mach-Scale Trailing Edge Flap Rotor’.. 57th Annual Forum, American Helicopter Society, 2001.
[15] Jacklin, S.A., Haber, A., de Simone, G., Norman, T.R., Kitaplioglu, C., Shinoda, P. “Full-Scale Wind Tunnel Test of an Individual Blade Control System for a UH-60.Helicopter”. 58th Annual Forum, American Helicopter Society, 2002.
[16] Straub, F.K., Kennedy, D.K., Stemple, A.D., Anand, V.R., Birchette, T.S. “Development and Whirl Tower Test of the SMART Active Flap Rotor”. SPIE Intl. Symposium on Smart Structures and Materials, San Diego CA. March 2004..
[17] Patt D., Chandrasekar J., Bernstein D., Friedmann P. HHC Control Algorithm Revisited. J. of Guidance and Control. v.28, No.5, 2005.
[18] Dieterich, O., Enenkl, B., Roth, D. “Trailing Edge Flaps for Active Rotor Control Aeroelastic Characteristics of the ADASYS Rotor System”. 62nd Annual Forum, American Helicopter Society. 2006.
[19] Maucher, C.K., Grohmann, B.A., Janker, P., Altmikus, A., .Jensen, F., Baier, H. “Actuator Design for the Active Trailing Edge of a Helicopter Rotor Blade”.. 33rd European Rotorcraft Forum, 2007.
[20] Kota, S., Ervin, G., Osborn, R., Ormiston, R.A. “Design and Fabrication of an Adaptive Leading Edge Rotor Blade”. 64th Annual Forum American Helicopter Society, 2008.
[21] Konstanzer, P., Enenkl, B., Aubourg, P.-A., Cranga, P. “Recent Advances in Eurocopter’s Passive and Active Vibration Control”. 64th Annual Forum, American Helicopter Society, 2008.
[22] Viswamurthy, S.R., Ganguli, R. “Optimal Placement of Piezoelectric Actuated Trailing-Edge Flaps for Helicopter Vibration Control”. J. Aircraft. v. 46, No.1,pp.244-253, 2009.
[23] Gennaretti, M., Molica Colella, M., Bernardini, G. “Analysis of Helicopter Vibratory Hub Loads Alleviation by Cyclic Trail-edge Blade Flap Actuation”. Aeronautical. J., v.113, No. 1146, pp. 549-556, 2009.
[24] Straub F. et al. “SMART Rotor Development and Wind-Tunnel Test”. 35th European Rotorcraft

Forum, 2009.
[25] Roget, B., Chopra, I. "Wind-Tunnel Testing of Rotor with Individually Controlled Trailing-Edge Flaps for Vibration Reduction". J. Aircraft. v.45, No.3, pp. 868-879, 2008.
[26] Ивчин В.А., Современная математическая модель для исследования динамики вертолета на пилотажных стендах, Научный вестник МГТУ ГА №125(1), ФА ВТ МГТУ ГА, Москва, 2008.
[27] Брамвелл А.Р., Динамика вертолетов. Москва, Машиностроение, 1985.
[28] Артамонов Б.Л., Влияние близости земли на аэродинамические характеристики несущего винта вертолета, в кн.: Проектирование вертолетов, Москва, МАИ, 1977.
[29] Шайдаков В.И., Артамонов Б.Л., Приближенный метод расчета аэродинамических характеристик несущего винта с типовым законом распределения циркуляции по радиусу лопасти, в кн.: Проблемы проектирование современных вертолетов, Москва, МАИ, 1980.
[30] Ивчин В.А., Метод представления экспериментальных нестационарных характеристик при продольных колебаниях профиля, в кн.: Задачи аэродинамики летательных аппаратов и их частей, Москва, МАИ, 1989.

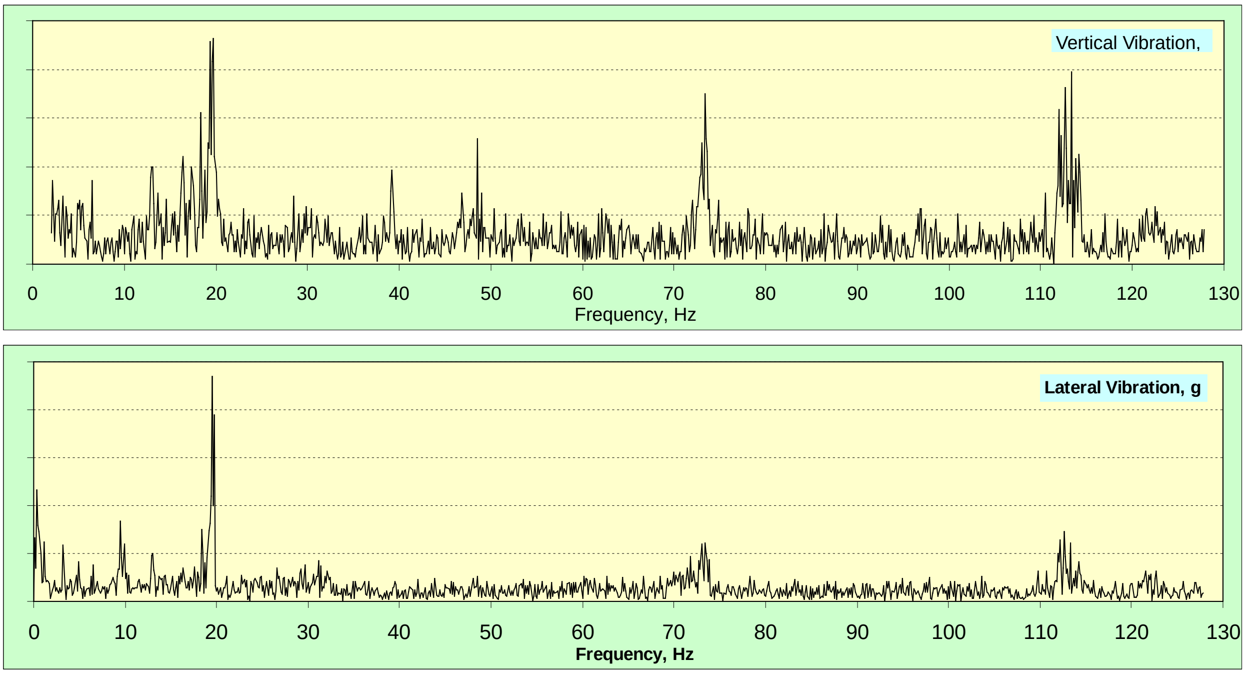

Figure 1.Vibration Spectra for a Helicopter with 6-Bladed Rotor (Flight Test)

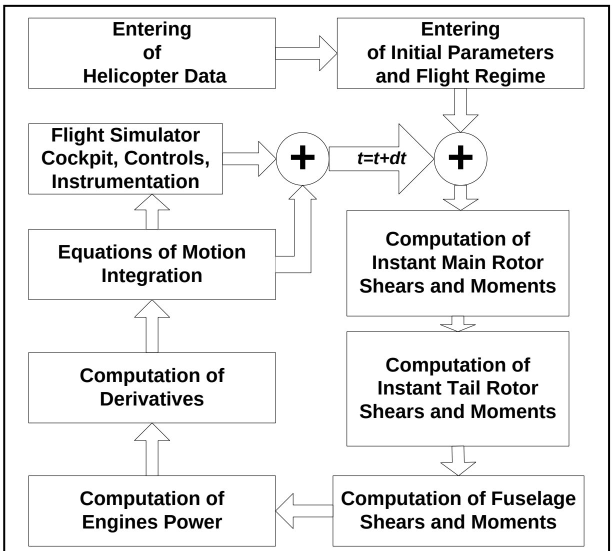

Figure 2. Structure of Helicopter Model

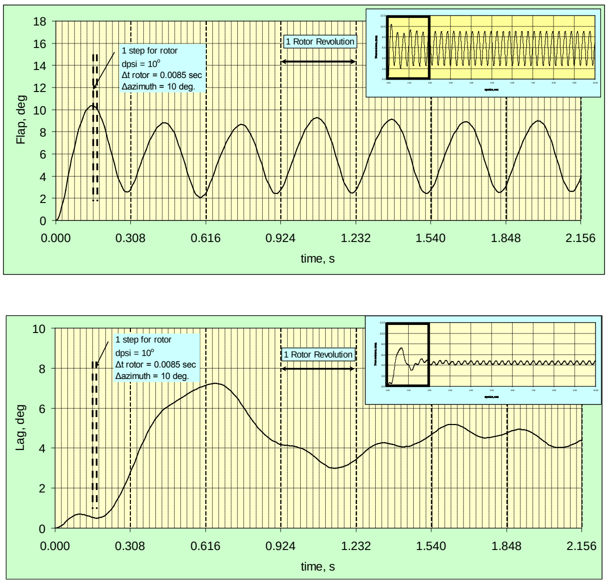

Figure 3. Time Histories of Blade Motion

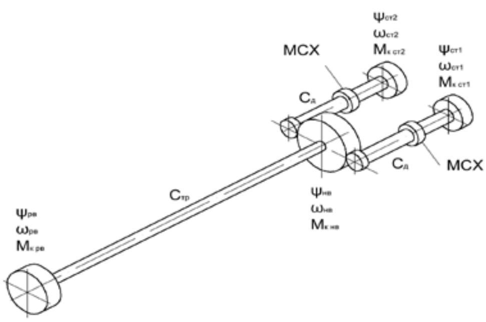

Notes:

Azimuth angles:
$\psi_{ст1}$, $\psi_{ст2}$ - free turbine 1, 2
$\psi_{НВ}$, $\psi_{рв}$ – main, tail rotor;

Angular rates:
$\omega_{ст1}$, $\omega_{ст2}$ – free turbine 1, 2
$\omega_{НВ}$, $\omega_{рв}$ – main, tail rotor;

Moments:
$M_{k\ ст1}$, $M_{k\ ст2}$ – free turbine 1, 2
$M_{k\ НВ}$, $M_{k\ рв}$ – main, tail rotor;

Elasticities:
$C_д$, $C_{тр}$ – engine, tail rotor shaft;

MCX – freewheeling clutch

Figure 4. Model of Helicopter Power Plant with Elastic Transmission

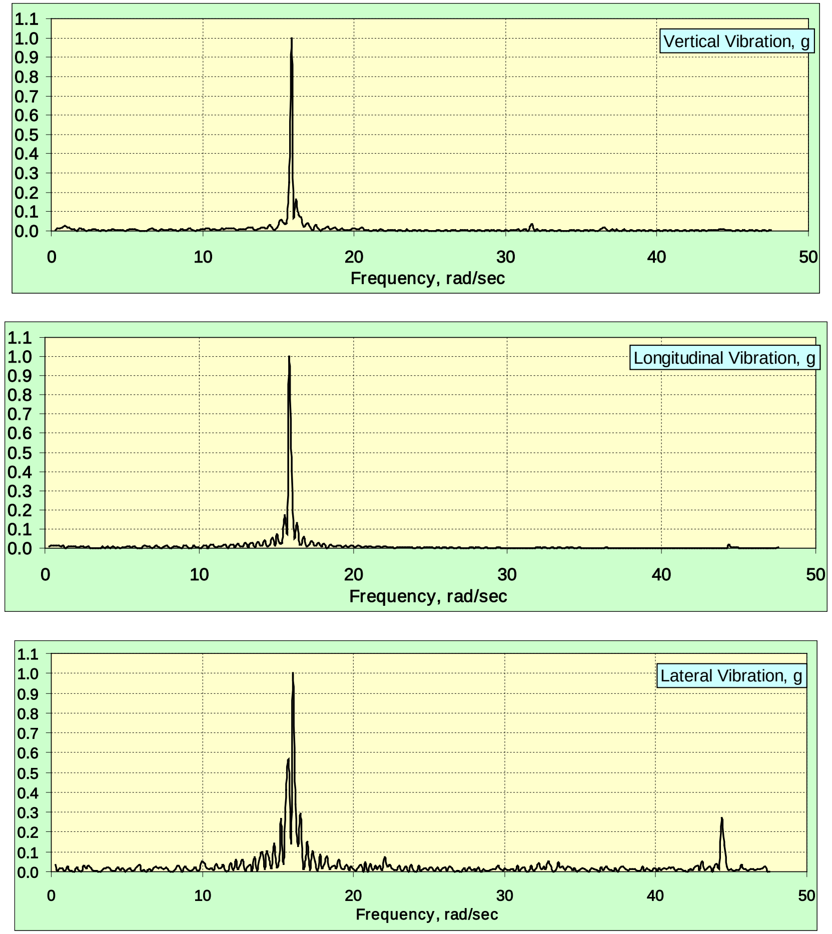

Figure 5. Vibration Spectra for Mi-8 Helicopter (Flight Simulator)

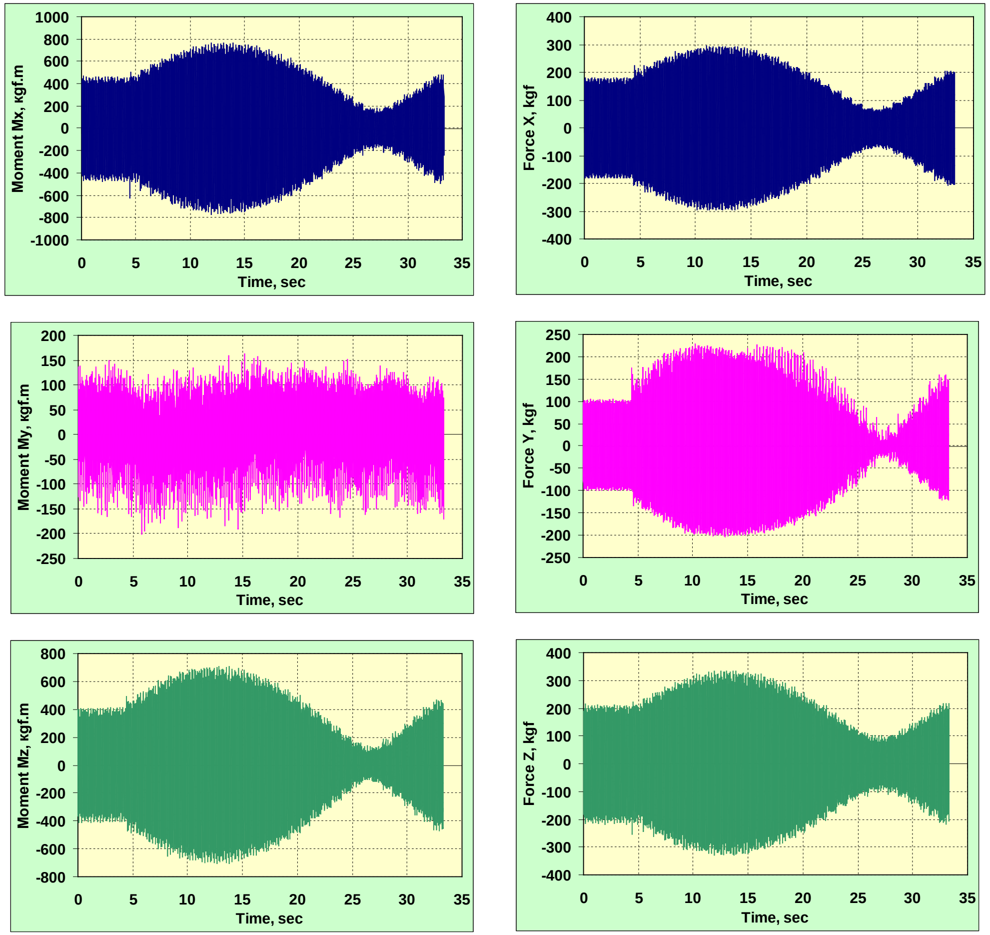

Figure 6. Airspeed 150 km/h, 4/rev Control, Amplitude 0.5 deg., Phase Change - Step 15 deg.

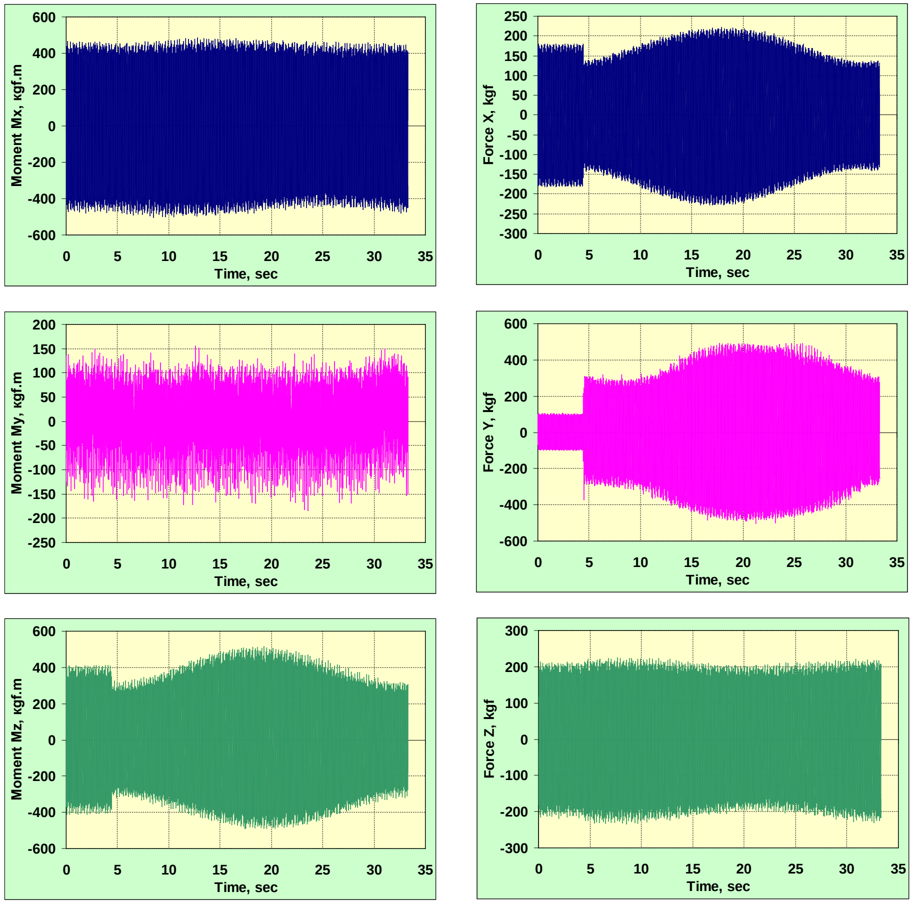

Figure 7. Airspeed 150 km/h, 5/rev Control, Amplitude 0.5 deg., Phase Change – Step 15 deg

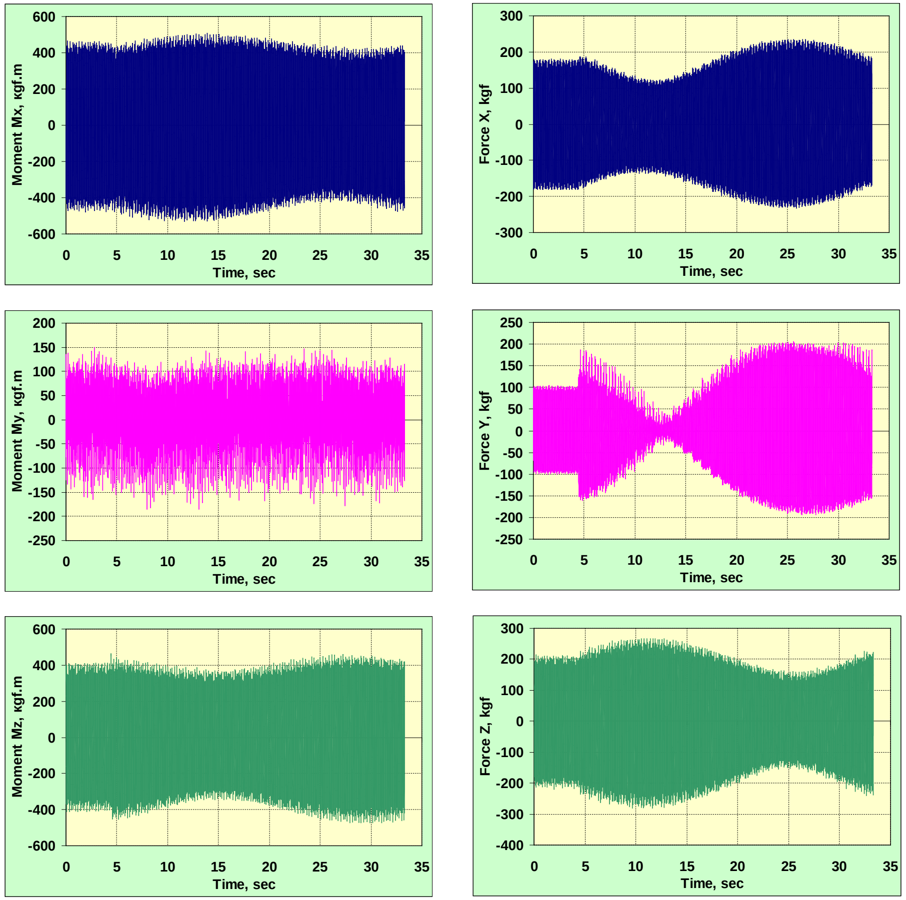

Figure 8 Airspeed 150 km/h, 6/rev Control, Amplitude 0.5 deg., Phase Change – Step 15 deg.

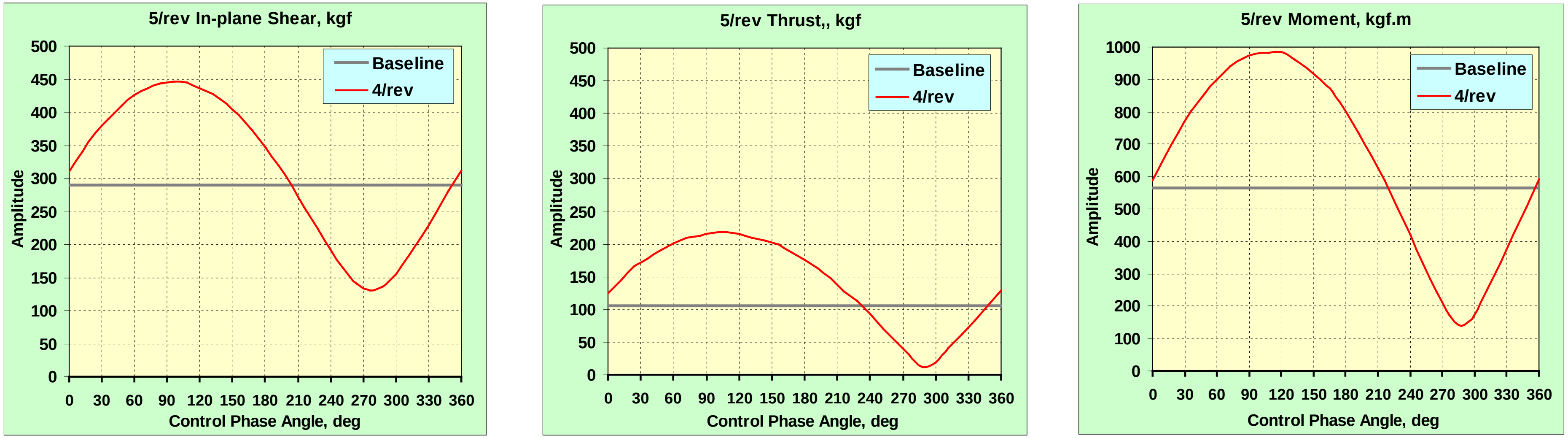

Figure 9. Airspeed 150 km/h, 4/rev Control, Amplitude 0.5 deg. Loads vs. Control Phase.

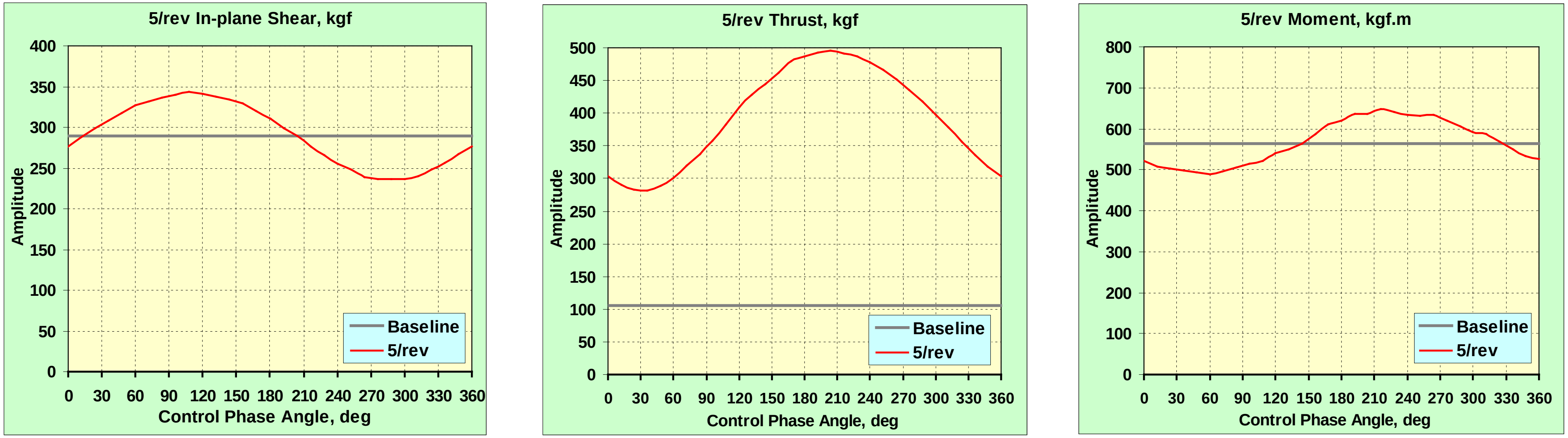

Figure 10. Airspeed 150 km/h, 5/rev Control, Amplitude 0.5 deg. Loads vs. Control Phase

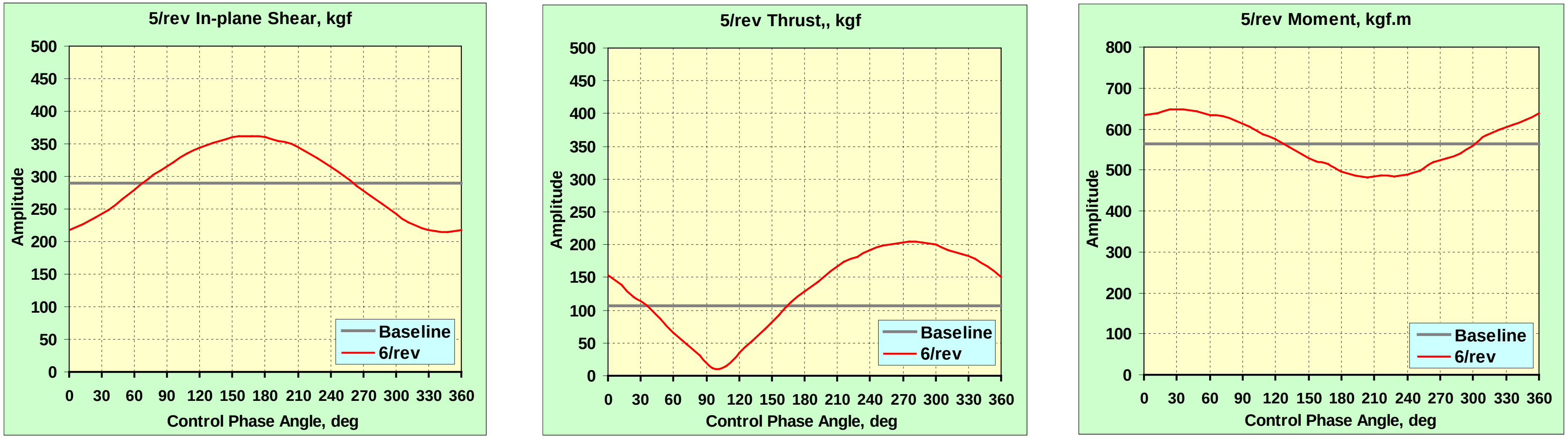

Figure 11. Airspeed 150 km/h, 6/rev Control, Amplitude 0.5 deg., Loads vs. Control Phase.

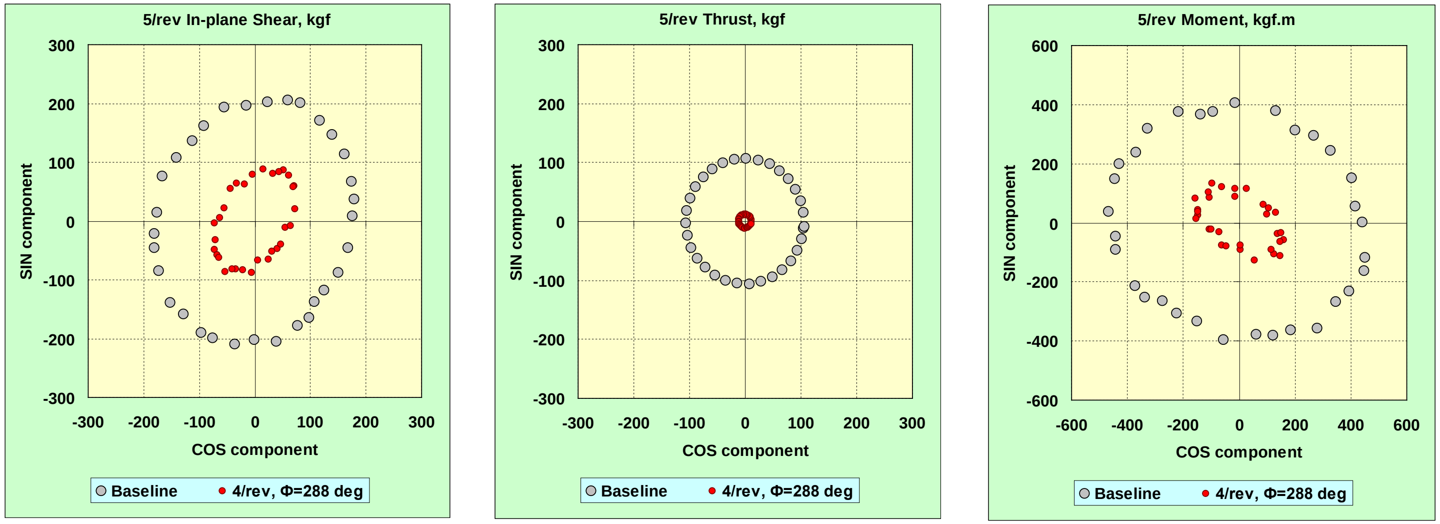

Figure 12. Airspeed150 km/h, Load Vectors Loci vs. Azimuth Angle. Baseline and 4/rev Control, Amplitude 0.5 deg., Phase 288 deg.

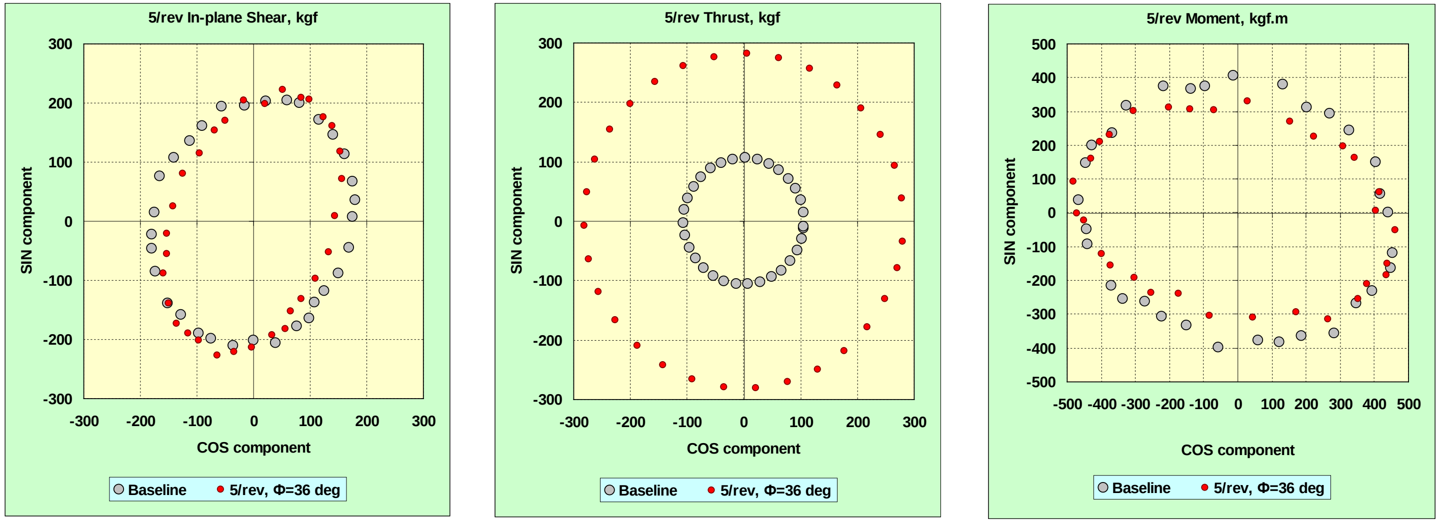

Figure 13. Airspeed 150 km/h, Load Vectors Loci vs. Azimuth Angle. Baseline and 5/rev Control, Amplitude 0.5 deg., Phase 36 deg.

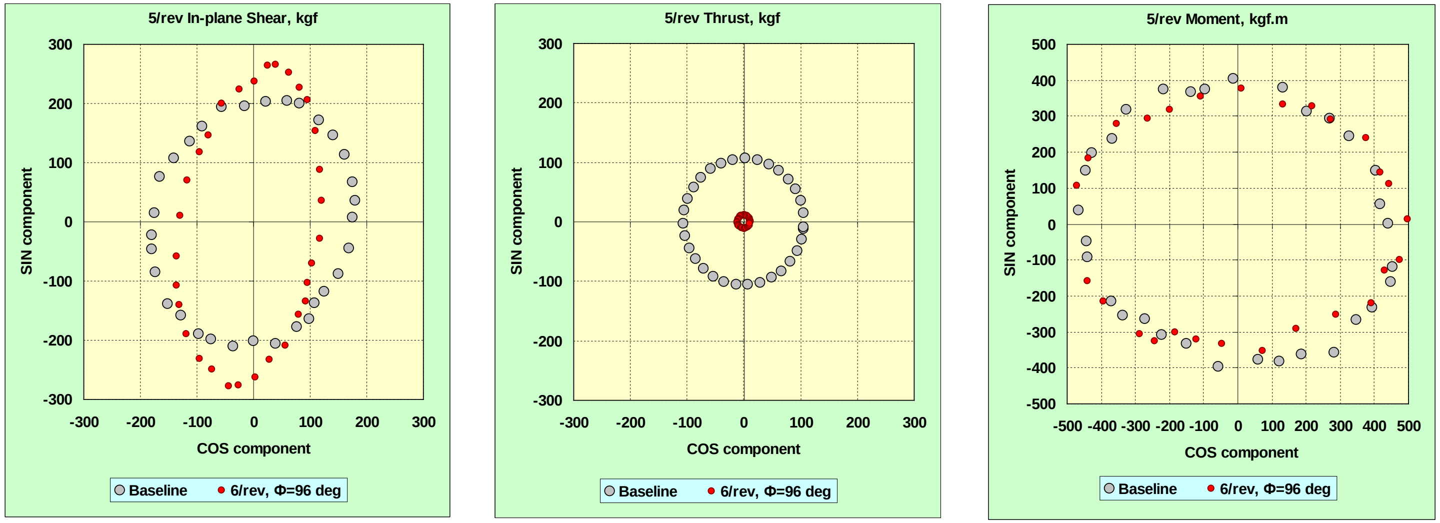

Figure 14. Airspeed 150 km/h, Load Vectors Loci vs. Azimuth Angle. Baseline and 6/rev Control, Amplitude 0.5 deg., Phase 96 deg.

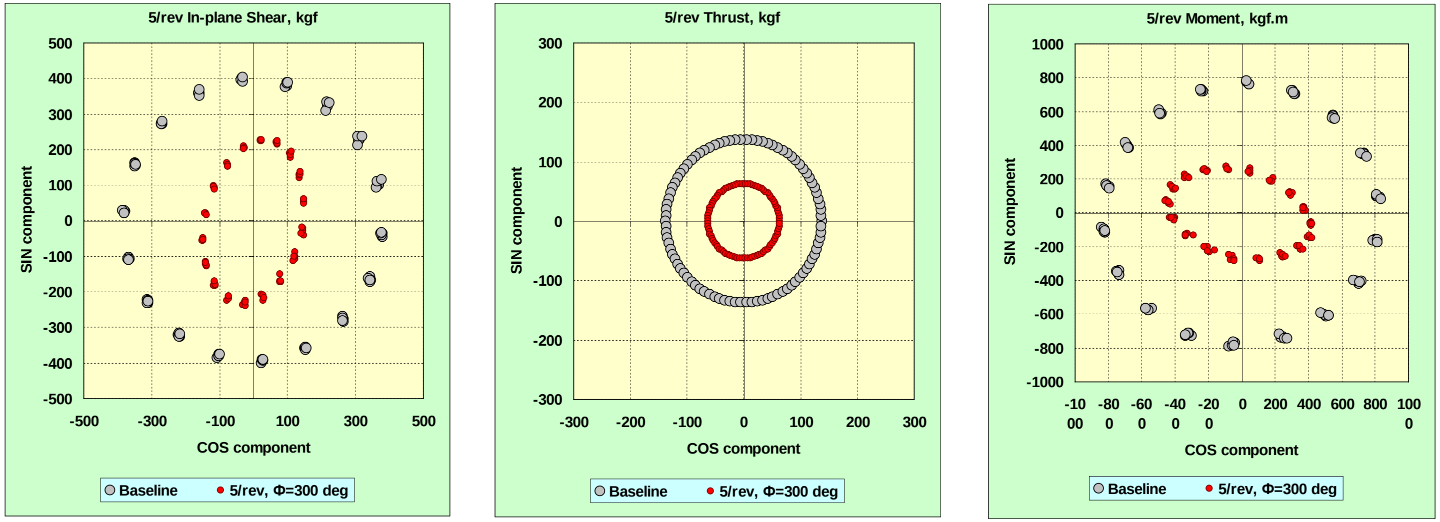

Figure 15. Airspeed 230 km/h, Load Vectors Loci vs. Azimuth Angle. Baseline and 4/rev Control, Amplitude 0.5 deg., Phase 300 deg.

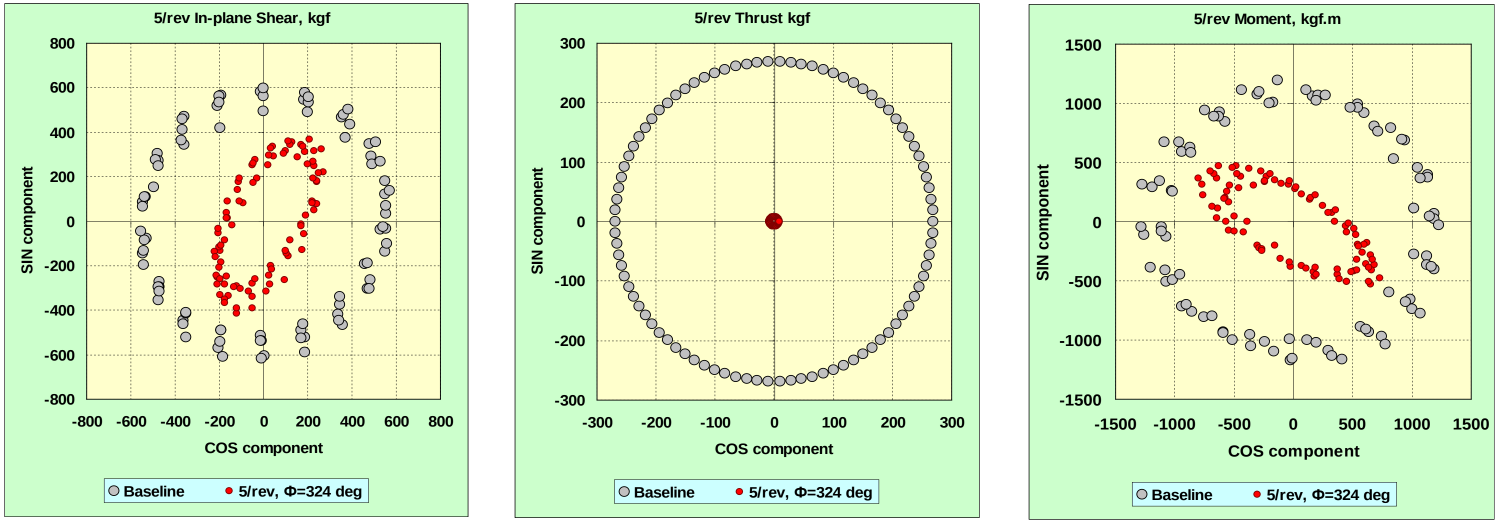

Figure 16. Airspeed 300 km/h, Load Vectors Loci vs. Azimuth Angle. Baseline and 4/rev Control, Amplitude 0.5 deg., Phase 324 deg.

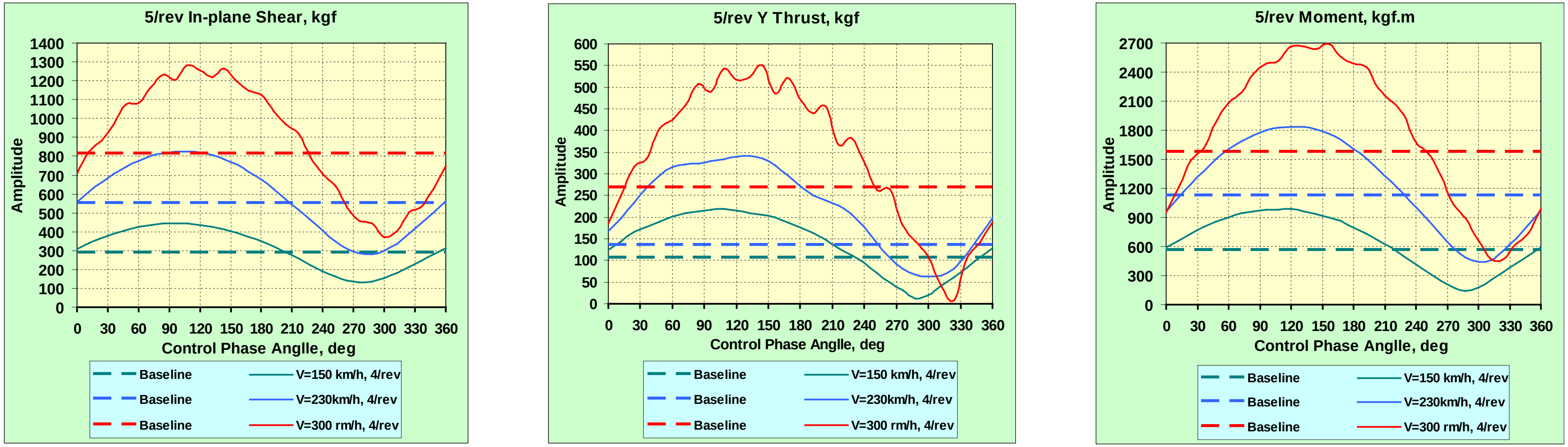

Figure 17. Loads vs. Control Phase. 4/rev Control, Amplitude 0.5 deg., Airspeeds 150, 230, and 300 km/h.

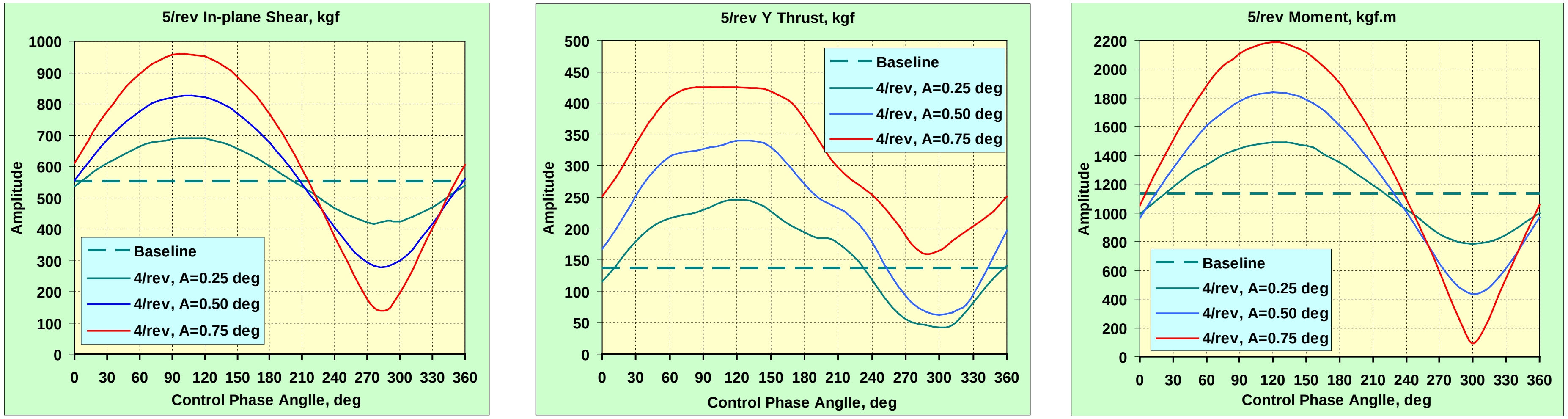

Figure 18. Loads vs. Control Phase. 4/rev Control, Airspeed 230 km/h , Amplitudes 0.25, 0.5, and 0.75 deg.

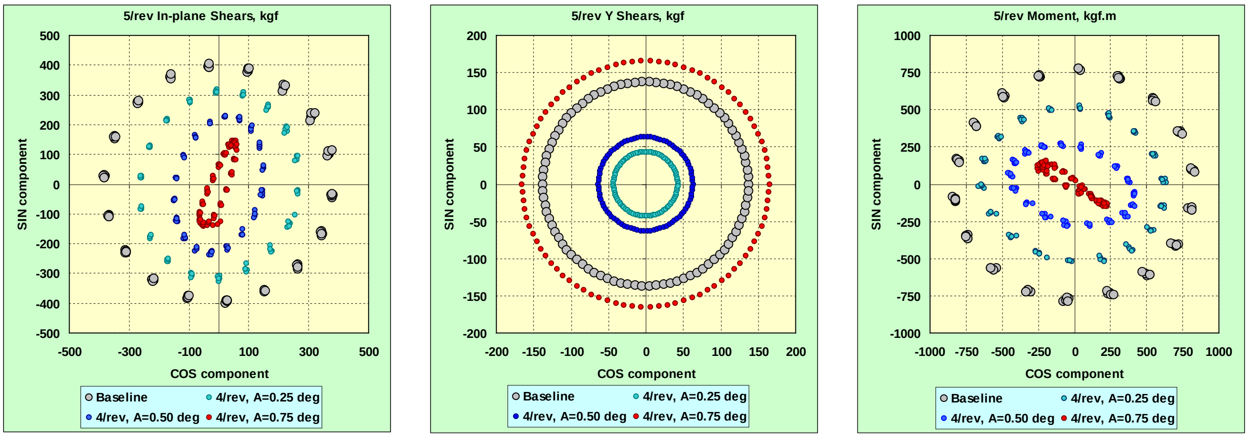

Figure 19. Airspeed 230 km/h, Load Vectors Loci vs. Azimuth Angle. Baseline and 4/rev Control, Amplitudes 0.25, 0.5,and 0.75 deg., Phase 300 deg.

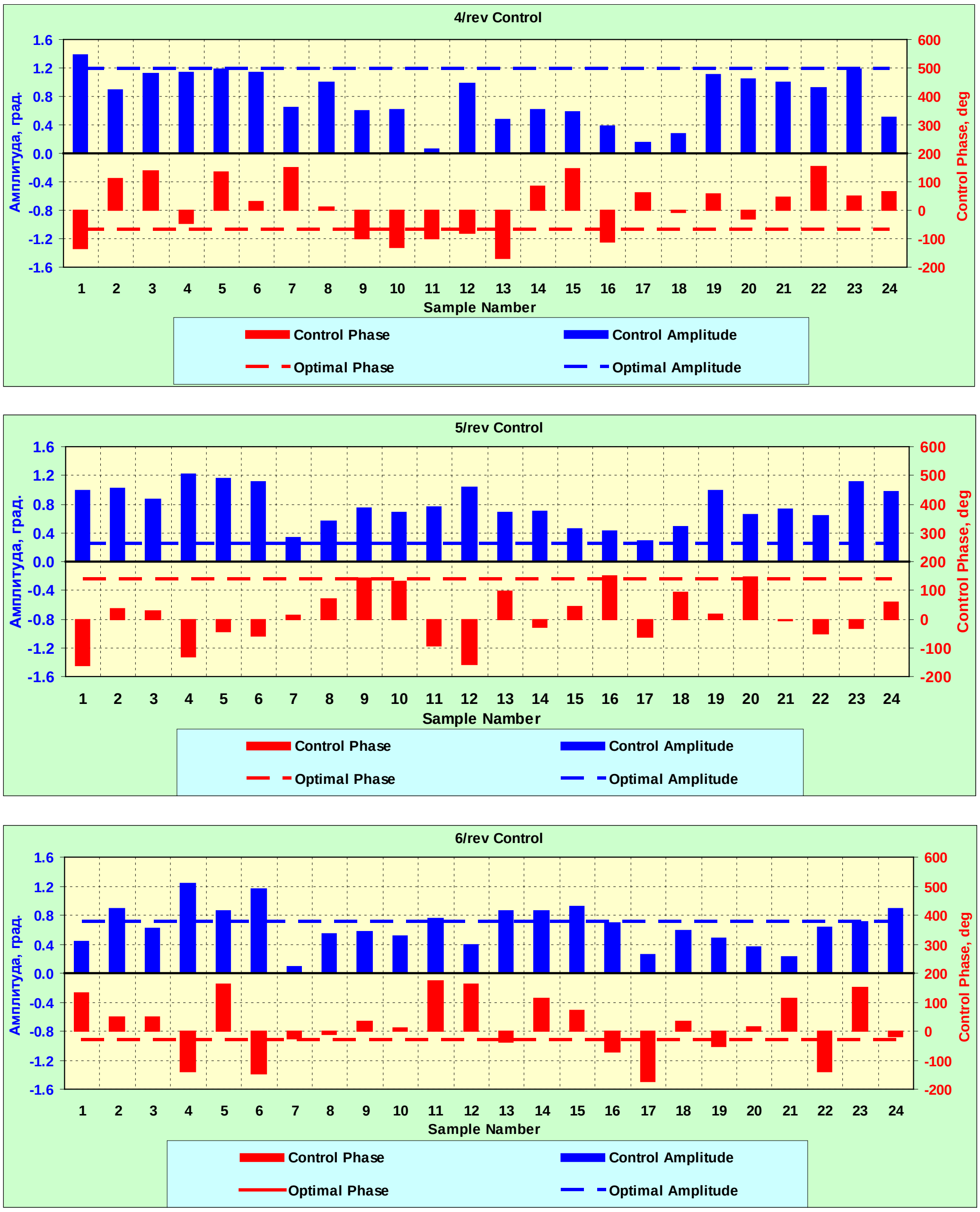

Figure 20. Airspeed 230 km/h. Random Input Samples for T-Matrix Determination

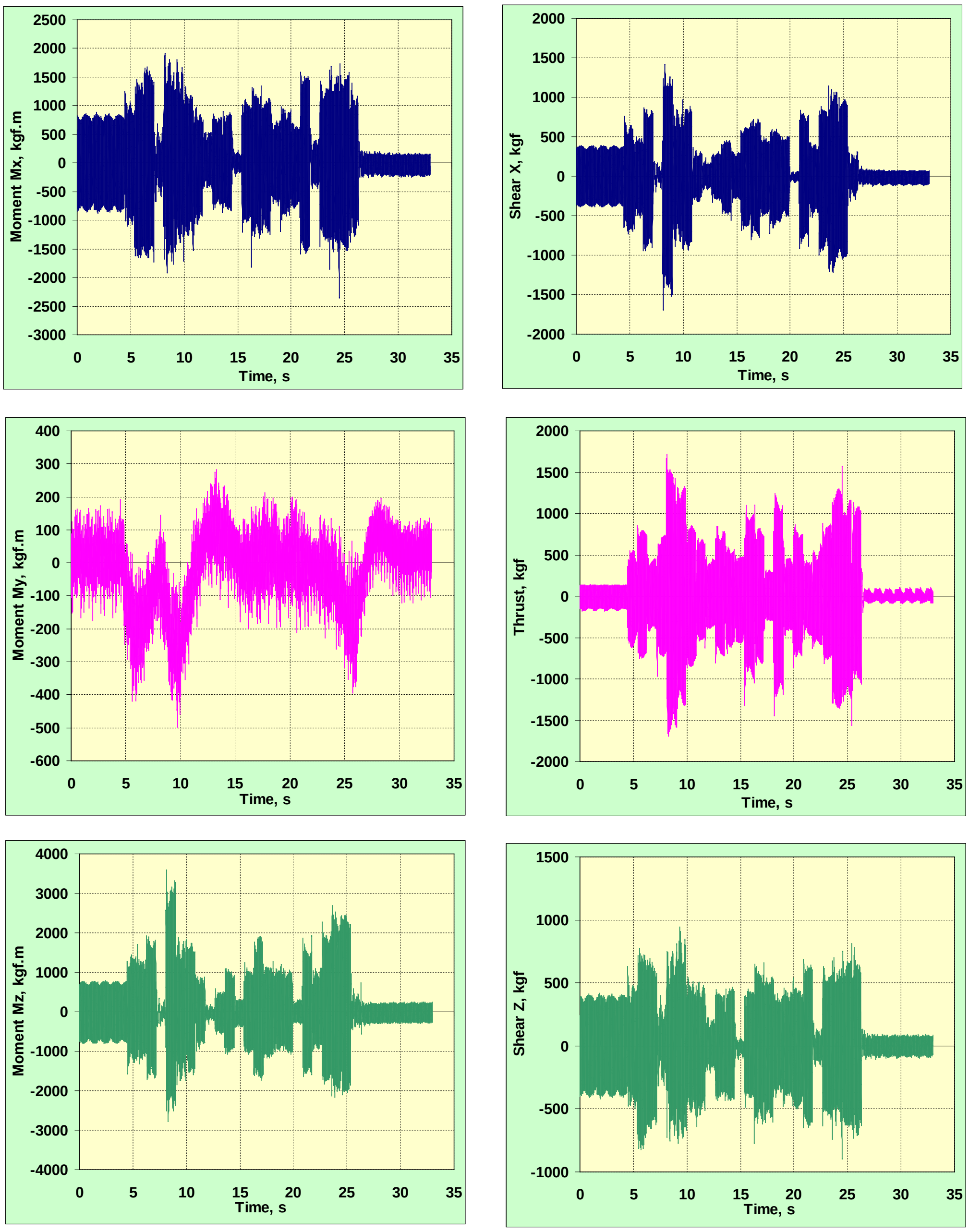

Figure 21. Airspeed 230 km/h. Time Histories for Loads Response: Baseline Case (0-4.5 sec), Random Input Samples for T-Matrix Determination (4.5-26.7 sec) and Optimal Control Application (26.7-33.0 sec).